A new method to determine large scale structure from the luminosity distance

2014 Class. Quantum Grav. 31 115008

(http://iopscience.iop.org/0264-9381/31/11/115008)

IOP Publishing Classical and Quantum Gravity
Class. Quantum Grav. **31** (2014) 115008 (16pp) doi:10.1088/0264-9381/31/11/115008

A new method to determine large scale structure from the luminosity distance

Antonio Enea Romano[1,2,3,4,5], **Hsu-Wen Chiang**[1,2,3] **and Pisin Chen**[1,2,3,6]

[1] Department of Physics, National Taiwan University, Taipei 10617, Taiwan, Republic of China
[2] Leung Center for Cosmology and Particle Astrophysics, National Taiwan University, Taipei 10617, Taiwan, Republic of China
[3] Graduate Institute of Astrophysics, National Taiwan University, Taipei 10617, Taiwan, Republic of China
[4] Department of Physics, McGill University, Montréal, QC H3A 2T8, Canada
[5] Instituto de Fisica, Universidad de Antioquia, A.A. 1226, Medellin, Colombia
[6] Kavli Institute for Particle Astrophysics and Cosmology, SLAC National Accelerator Laboratory, Menlo Park, CA 94025, USA

E-mail: enea@hep.physics,mcgill.ca

Received 1 January 2014, revised 4 April 2014
Accepted for publication 22 April 2014
Published 20 May 2014

Abstract

The luminosity distance can be used to determine the properties of large scale structure around the observer. To this purpose we develop a new inversion method to map luminosity distance to a Lemaitre–Tolman–Bondi (LTB) metric based on the use of the exact analytical solution for Einstein equations. The main advantages of this approach are an improved numerical accuracy and stability, an exact analytical setting of the initial conditions for the differential equations which need to be solved and the validity for any sign of the functions determining the LTB geometry. Given the fully analytical form of the differential equations, this method also simplifies the calculation of the red-shift expansion around the apparent horizon point where the numerical solution becomes unstable. We test the method by inverting the supernovae Ia luminosity distance function corresponding to the best fit ΛCDM model. We find that only a limited range of initial conditions is compatible with observations, or a transition from red to blue-shift can occur at relatively low red-shift. Despite LTB solutions without a cosmological constant have been shown not to be compatible with all different set of available observational data, those studies normally fit data assuming a special functional ansatz for the inhomogeneity profile, which often depend only on few parameters. Inversion methods on the contrary are able to fully explore the freedom in fixing the functions which

determine a LTB solution. Another important possible application is not about LTB solutions as cosmological models, but rather as tools to study the effects on the observations made by a generic observer located in an inhomogeneous region of the Universe where a fully non perturbative treatment involving exact solutions of Einstein equations is required.

Keywords: luminosity distance, large scale structure, inhomogeneous cosmological models
PACS number: 98.80.Es

1. Introduction

When different cosmological data [1–8] are interpreted using FLRW models a dominant dark energy must be introduced. Since the nature of dark energy is not well understood, there has been some efforts to look for alternative explanations based on relaxing the hypothesis of large scale homogeneity. It is well known that inhomogeneous matter dominated models can fit some of the available observations [9–30], and different methods have been developed to solve the inversion problem (IP) to map a given observed luminosity distance function $D_L(z)$ to the corresponding inhomogeneous metric. In this paper we will study the case of a radially inhomogeneous spherically symmetric pressureless solution, described by a Lemaitre–Tolman–Bondi (LTB) solution, assuming a central location of the observer. This is an open violation of the Copernican principle, but since this is more a philosophical principle than a fully observationally established fact, it is worth investigation this type of cosmological model. Previous solutions to the IPs [10, 31] were based on the solution of the radial light cone geodesics using a different system of coordinates, but they all required a numerical integration of the background Einstein's equations, while in this paper we derive a fully analytical method for the solution of the IP, based on the use of the exact analytical solution.

Another interesting approach to the IP [11, 32, 33] makes use of the Dyer–Roeder equation, which is based on the approximation that the shear factor σ is negligible, and requires to specify an additional function $\alpha(z)$, which gives the fraction of matter density that is smoothly distributed. This is not exactly the same IP we are solving, since we use the actual expression for the angular diameter distance $D_A(z)$ in LTB spaces, without any additional simplifying assumption such as neglecting the shear, which is implicit in the use of the Dyer–Roeder equation, or the need to of specifying a new function such as $\alpha(z)$. The inversion equations obtained using this method in general still have a numerical instability problem at the point z_c where $D_A(z)$ reaches its maximum, but with an appropriate choice of the initial conditions this can be avoided, with the limitation of solving the problem only for a certain value of the initial conditions. Nevertheless, since this is just an apparent horizon, a solution can be found for any value of the initial conditions, and in fact this is what we are able to do by expanding the solution around z_c. In this regard our method is more general since it is able to overcome the apparent horizon for an arbitrary set of initial conditions. We find that some of the initial conditions are incompatible with observational data since they lead to a contraction of the universe, but this is not related to the presence of a numerical instability in the differential equations at z_c, which our method is always able to overcome making it more general and allowing in fact to find not just one solution but a class of solutions corresponding to the different possible choices of initial conditions.

The use of galaxy number counts [26] has also been proposed to distinguish between inhomogeneous models and ΛCDM using both analytical and numerical approaches

[12, 20, 31]. CMB observations in the context of on inhomogeneous models need a careful treatment as observed in [34, 35], since the inhomogeneous radiation component could have important effects respect to the approximation of having only an inhomogeneous matter component.

There has also been a considerable interest on the effects of large scale inhomogeneities in presence of dark energy [36–41]. More recently there has been some evidence that LTB solutions cannot provide a fully consistent cosmological model compatible with all available observations [42, 43]. These studies are nevertheless based on fitting experimental data with some particular functional ansatz for the functions defining the model, and as such they do not explore the full space of all possible inhomogeneity profiles. The numerical inversion approach adopted in the present paper is on the contrary able to explore the full range of all the possible LTB solutions and initial conditions. It should observed that the IP we study in this paper is based on imposing some very strict constraints since we reproduce exactly the theoretical ΛCDM theoretical prediction, while fitting actual observational data [44], due to their intrinsic noise, can lead to much less stringent constraints on the inhomogeneous model. Since the inversion equations are numerically unstable around the red-shift corresponding to the maximum of the angular diameter distance, a local Taylor expansion is necessary around that point, for which our fully analytical version of differential equations is particularly suitable. Our approach provides a local Taylor expansion of the solution at any point, and the numerical solution of the differential equations is more stable since we don't need to integrate numerically the background equations. The use of the analytical solution allows also to set exactly the necessary initial conditions, while in previous attempts [10] it was necessary to derive some approximate consistency condition. As a result we can get a more accurate solution of the IP, and we are also able to explore the full class of LTB models with an arbitrary value of the central curvature in a self-consistent way. We apply this method to invert the theoretical luminosity distance function corresponding to the best find ΛCDM parameters and find that only a certain range of central of initial conditions is allowed, since for other models a transition from red to blue-shift occurs, making these models incompatible with the observed luminosity distance. We also show that the value of the Hubble parameter at the last scattering surface is independent of the central value of the curvature, and differ by about 20% from the best fit ΛCDM value as constrained by CMB observations. This confirms the necessity to introduce a bang function to fit CMB data with LTB models, but contrary to previous numerical inversion studies it shows it independently of the central value of the functions defining the LTB model, by exploring the full class of possible initial conditions.

The method we developed does not need to be applied to LTB metrics as cosmological models describing the local universe around us, but could be applied to study the effects of large scale inhomogeneities for a generic observer located inside some region of the Universe corresponding to a local overdensity or underdensity which cannot be modeled simply perturbation of a FLRW metric.

2. Lemaitre–Tolman–Bondi (LTB) Solution

LTB solution can be written as [45–47]

$$\mathrm{d}s^2 = -\mathrm{d}t^2 + \frac{(R_{,r})^2 \mathrm{d}r^2}{1+2E} + R^2 \mathrm{d}\Omega^2, \tag{1}$$

where R is a function of the time coordinate t and the radial coordinate r, $R = R(t, r)$, E is an arbitrary function of r, $E = E(r)$ and $R_{,r} = \partial R/\partial r$.

Einstein's equations give

$$\left(\frac{\dot{R}}{R}\right)^2 = \frac{2E(r)}{R^2} + \frac{2M(r)}{R^3}, \tag{2}$$

$$\rho(t,r) = \frac{2M_{,r}}{R^2 R_{,r}}, \tag{3}$$

with $M = M(r)$ being an arbitrary function of r and the dot denoting the partial derivative with respect to t, $\dot{R} = \partial R(t,r)/\partial t$. The solution of equation (2) can be expressed parametrically in terms of a time variable $\eta = \int^t \mathrm{d}t'/R(t',r)$ as

$$\tilde{R}(\eta,r) = \frac{M(r)}{-2E(r)}[1 - \cos(\sqrt{-2E(r)}\eta)], \tag{4}$$

$$t(\eta,r) = \frac{M(r)}{-2E(r)}\left[\eta - \frac{1}{\sqrt{-2E(r)}}\sin(\sqrt{-2E(r)}\eta)\right] + t_b(r), \tag{5}$$

where $\tilde{R}$ has been introduced to make clear the distinction between the two functions $R(t,r)$ and $\tilde{R}(\eta,r)$ which are trivially related by

$$R(t,r) = \tilde{R}(\eta(t,r),r), \tag{6}$$

and $t_b(r)$ is another arbitrary function of r, called the bang function, which corresponds to the fact that big-bang/crunches can happen at different times. This inhomogeneity of the location of the singularities is one of the origins of the possible causal separation [9] between the central observer and the spatially averaged region for models with positive a_D.

We introduce the variables

$$a(t,r) = \frac{R(t,r)}{r}, \quad k(r) = -\frac{2E(r)}{r^2}, \quad \rho_0(r) = \frac{6M(r)}{r^3}, \tag{7}$$

so that the Einstein equations (2) and (3) are written in a form similar to those for FLRW models,

$$\mathrm{d}s^2 = -\mathrm{d}t^2 + a^2\left[\left(1 + \frac{a_{,r}\,r}{a}\right)^2 \frac{\mathrm{d}r^2}{1 - k(r)r^2} + r^2\mathrm{d}\Omega_2^2\right], \tag{8}$$

$$\left(\frac{\dot{a}}{a}\right)^2 = -\frac{k(r)}{a^2} + \frac{\rho_0(r)}{3a^3}, \tag{9}$$

$$\rho(t,r) = \frac{(\rho_0 r^3)_{,r}}{3a^2r^2(ar)_{,r}}. \tag{10}$$

The solution of equations (4) and (5) can now be written as

$$\tilde{a}(\tilde{\eta},r) = \frac{\rho_0(r)}{6k(r)}[1 - \cos(\sqrt{k(r)}\,\tilde{\eta})], \tag{11}$$

$$t(\tilde{\eta},r) = \frac{\rho_0(r)}{6k(r)}\left[\tilde{\eta} - \frac{1}{\sqrt{k(r)}}\sin(\sqrt{k(r)}\,\tilde{\eta})\right] + t_b(r), \tag{12}$$

where $\tilde{\eta} \equiv \eta\, r = \int^t \mathrm{d}t'/a(t',r)$.

In the rest of paper we will use this last set of equations and drop the tilde to make the notation simpler. Furthermore, without loss of generality, we may set the function $\rho_0(r)$ to be a constant, $\rho_0(r) = \rho_0 =$ constant.

3. Geodesic equations

The luminosity distance for an observer at the center of a LTB space as a function of the red-shift is given by

$$D_L(z) = (1+z)^2 R(t(z), r(z)) = (1+z)^2 r(z) a(\eta(z), r(z)), \tag{13}$$

where $(t(z), r(z))$ or $((\eta(z), r(z))$ is the solution of the radial null geodesic equations. The past-directed radial null geodesic is given by

$$\frac{\mathrm{d}T(r)}{\mathrm{d}r} = f(T(r), r), \quad f(t, r) = \frac{-R_{,r}(t, r)}{\sqrt{1+2E(r)}}, \tag{14}$$

where $T(r)$ is the time coordinate along the geodesic as a function of the coordinate r. Applying the definition of red-shift it is possible to obtain [48]:

$$\frac{\mathrm{d}\eta}{\mathrm{d}z} = \frac{\partial_r t(\eta, r) - F(\eta, r)}{(1+z)\partial_\eta F(\eta, r)} = p(\eta, r), \tag{15}$$

$$\frac{\mathrm{d}r}{\mathrm{d}z} = -\frac{a(\eta, r)}{(1+z)\partial_\eta F(\eta, r)} = q(\eta, r), \tag{16}$$

where we have used

$$f(t(\eta, r), r) = F(\eta, r), \tag{17}$$

$$\dot{f}(t(\eta, r), r) = \frac{1}{a}\partial_\eta F(\eta, r), \tag{18}$$

$$R_{,r}(t, r) = \partial_r R(t(\eta, r), r) + \partial_\eta R(t(\eta, r), r)\partial_r \eta, \tag{19}$$

$$\begin{aligned} F(\eta, r) &= -\frac{1}{\sqrt{1-k(r)r^2}}[\partial_r(a(\eta, r)r) + \partial_\eta(a(\eta, r)r)\partial_r\eta] \\ &= -\frac{1}{\sqrt{1-k(r)r^2}}[\partial_r(a(\eta, r)r) - \partial_\eta(a(\eta, r)r)a(\eta, r)^{-1}\partial_r t]. \end{aligned} \tag{20}$$

The functions p, q, F have an explicit analytical form which can be obtained from $a(\eta, r)$ and $t(\eta, r)$. Using this approach the coefficients of equations (15) and (16) are fully analytical, which is a significant improvement over previous methods which required a numerical integration of the Einstein's equations to obtain the function $R(t, r)$. This version of the geodesics equations is suitable for both numerical and analytical applications, in particular will be useful to obtain a red-shift expansion of the inversion equations around the apparent horizon point.

4. Initial conditions

Before deriving the set of differential equations for the solution of the IP it is important to analyze how many independent initial conditions we need to fix. Our final goal will be to set and solve a set of differential equations in red-shift space starting from the center, where by definition $z = 0$. Given our choice of coordinates the model will be fully determined by the functions $k(z)$, $r(z)$, $\eta(z)$, corresponding to three initial conditions

$$\begin{aligned} r(0) &= 0 \\ \eta(0) &= \eta_0 \\ k(0) &= k_0. \end{aligned} \tag{21}$$

The system of differential equation we will derive only involves derivatives of order one respect to the red-shift, so these initial conditions will be enough. Given the assumption of the central location of the observer we have $r_0 = 0$, while the observed value of the Hubble parameter H_0 corresponds to another constraint among the central values k_0, η_0, so only one of them is independent. After defining the Hubble rate as

$$H^{\mathrm{LTB}} = \frac{\partial_t a(t,r)}{a(t,r)} = \frac{\partial_\eta a(\eta,r)}{a(\eta,r)^2} \tag{22}$$

we need to impose the two following conditions

$$a(\eta_0, 0) = a_0, \tag{23}$$

$$H^{\mathrm{LTB}}(\eta_0, 0) = H_0, \tag{24}$$

where a_0 is, as expected, an arbitrary parameter, η_0 is the value of the generalized conformal time coordinate η corresponding to the central observer today, and H_0 is the observed value of the Hubble parameter.

After re-writing the solution in terms of the following more convenient dimensionless quantities [18]

$$a(T,r) = \frac{a_0 \Omega_M^0 \sin^2\left(\frac{1}{2}T\sqrt{K(r)}\right)}{K(r)}, \tag{25}$$

$$t(T,r) = H_0^{-1}\frac{\Omega_M^0}{2K(r)}\left[T - \frac{1}{\sqrt{K(r)}}\sin(\sqrt{K(r)}T)\right] + t_b(r), \tag{26}$$

$$k(r) = (a_0 H_0)K(r), \tag{27}$$

$$\eta = T(a_0 H_0)^{-1}, \tag{28}$$

$$\rho_0 = 3\Omega_m^0 a_0^3 H_0^2, \tag{29}$$

we can solve equations (23), (24) for Ω_M^0 and T_0 to finally get the initial conditions and the exact solution in this form

$$a(T,r) = \frac{a_0(K_0+1)\sin^2\left(\frac{1}{2}T\sqrt{K(r)}\right)}{K(r)}, \tag{30}$$

$$t(T,r) = H_0^{-1}\frac{1+K_0}{2K(r)}\left[T - \frac{1}{\sqrt{K(r)}}\sin(\sqrt{K(r)}T)\right] + t_b(r), \tag{31}$$

$$K_0 = K(0), \tag{32}$$

$$T_0 = \frac{\arctan\left(2\sqrt{K_0}\right)}{\sqrt{K_0}} \tag{33}$$

$$\Omega_m^0 = K_0 + 1. \tag{34}$$

Since we have three unknown $\{\Omega_M^0, T_0, K_0\}$ and two constraints given by equations (23), (24), one of them can always remain free, and the other two can be expressed in terms of it. In this paper we have chosen K_0 to be the free parameter, but we could equivalently chose another one. The above form of the solution is particularly useful to explore the full class of LTB

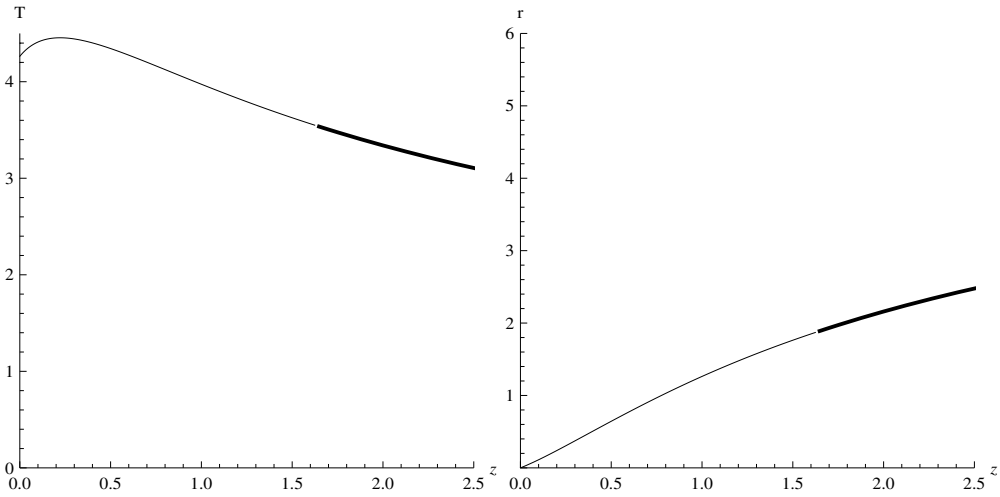

Figure 1. The conformal time $T(z)$ and the radial coordinate $r(z)$ are plotted as a function of red-shift for $K_0 = -0.9376$. The thick line correspond to the part after the apparent horizon.

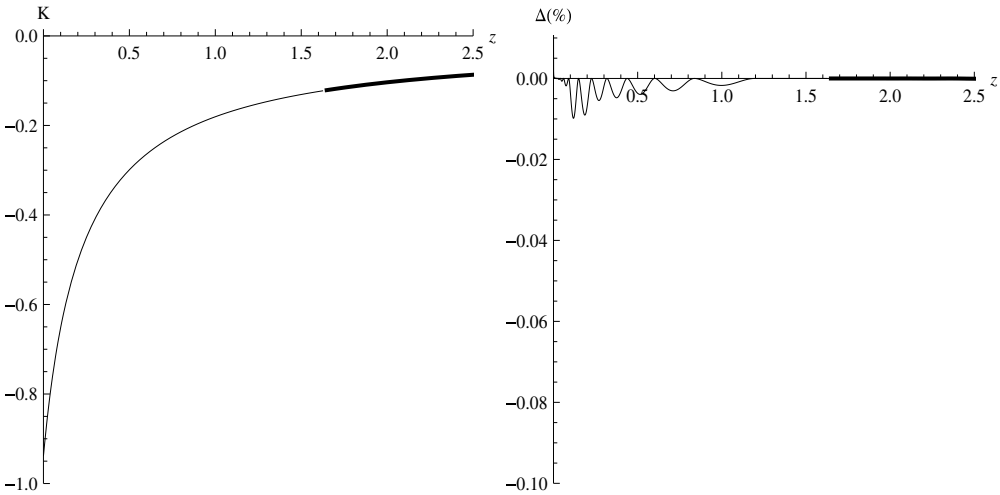

Figure 2. The curvature function $K(z)$ and the relative percentual $\Delta(z) = 100\frac{D^{\Lambda CDM}(z)-D^{\rm LTB}(z)}{D^{\Lambda CDM}(z)}$ error between the luminosity distance $D^{\Lambda CDM}(z)$ used as input and $D_L^{\rm LTB}(z)$ obtained by substituting the numerical solution of the differential equations for the inversion method are plotted as functions of red-shift for $K_0 = -0.9376$. The thick lines correspond to the part after the apparent horizon.

models since K_0 is a free parameter which determines through equation (33) the central value of the generalized dimensionless conformal time variable T_0. H_0 is also a free parameter which can be set according to observations and fixes the scale for the definition of the dimensionless quantities $K(r)$, T, Ω_m^0. This means that we can arbitrarily fix K_0 and H_0 as long as we impose the correct initial condition given by equations (33)–(34).

As expected a_0 does not appear in observable quantities such as the cosmic time $t(\eta, r)$, and it can be fixed to 1. It can be easily checked that the above solution is by construction in

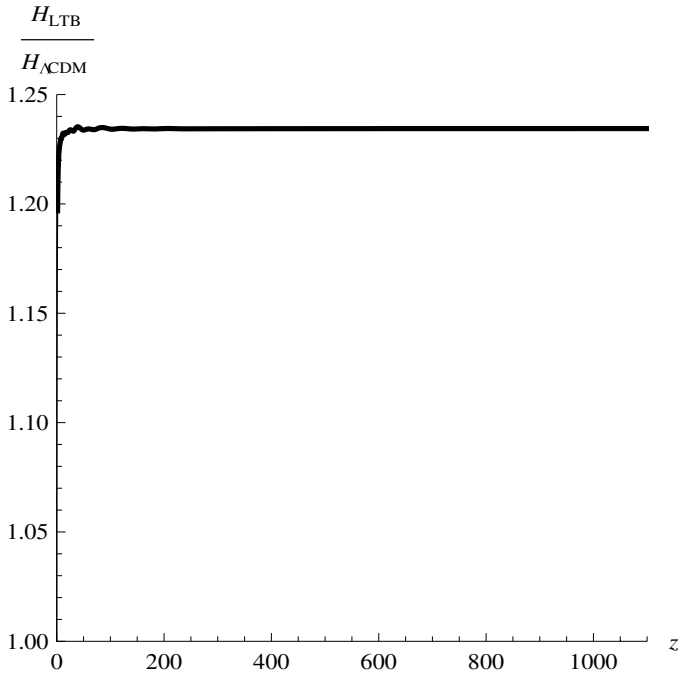

Figure 3. The ratio between the Hubble parameter $H^{\rm LTB}(z)$ and $H^{\Lambda CDM}(z)$ is plotted as function of the red-shift for $K_0 = -0.9376$. The thick lines correspond to the part after the apparent horizon.

agreement with any given value of H_0

$$H_0^{\rm LTB} = \frac{\partial_t a(t_0,0)}{a(t_0,0)} = \frac{\partial_\eta a(\eta_0,0)}{a(\eta_0,0)^2} = (a_0 H_0)\frac{\partial_T a(T_0,0)}{a(T_0,0)^2} = H_0, \tag{35}$$

and for any K_0 we can now determine the corresponding initial condition $T_0 = T(z=0)$. In this way we can self-consistently determine all the necessary initial conditions and we are left with the freedom to fix K_0 arbitrarily. As we will see later only some values of K_0 are consistent with observations. Our general approach to determine the initial conditions will allow us to explore the full class of LTB models, while in previous studies the value of K_0 has been fixed [10], and the initial conditions were based on some approximate consistency relation.

5. Inversion method differential equations

In the previous section we have seen that it is possible to derive a fully analytical set of radial null geodesics equations. Our goal now is to use these equations to obtain a new set of differential equations to map an observed $D_L(z)$ to a LTB model. In principle we need are three independent functions to fully specify a LTB solution, $M(r), k(r), t_b(r)$, but because of the freedom in fixing the radial coordinate only two of them are really independent. As explained in the previous sections we adopt the coordinates system in which $M(r) \propto r^3$, so that only $k(r), t_b(r)$ are left to be determined. In this paper we will consider the case in which $t_b(r) = 0$, since we are inverting only one observable, the luminosity distance $D_L(z)$, and the inversion method will be enough to fully determine the remaining function $k(z)$, and then $k(r)$. We will leave to a future work the case in which an additional red-shift dependent observable is included, which will then require to also develop an inversion method for $t_b(r)$. In the

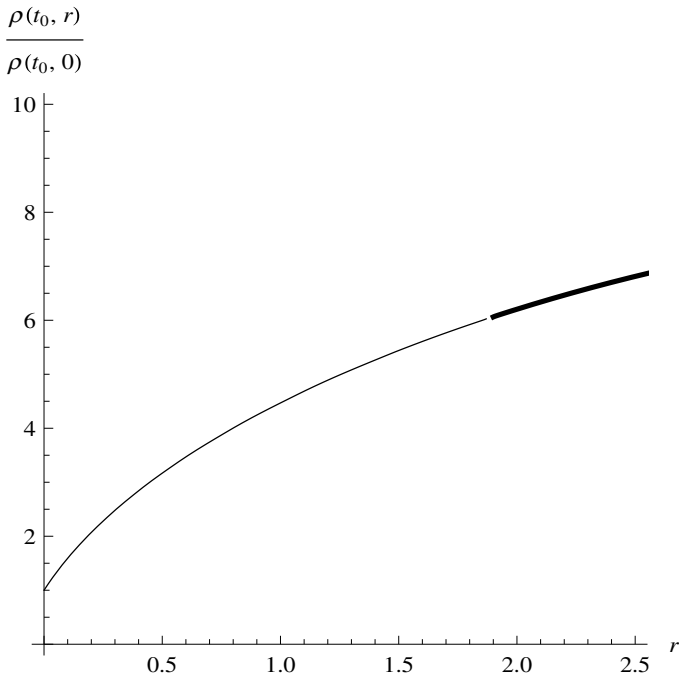

Figure 4. The energy density profile $\frac{\rho(r,t_0)}{\rho(r\to 0,t_0)}$ is plotted as function of the comoving radius for $K_0 = -0.9376$. The thick lines correspond to the part after the apparent horizon.

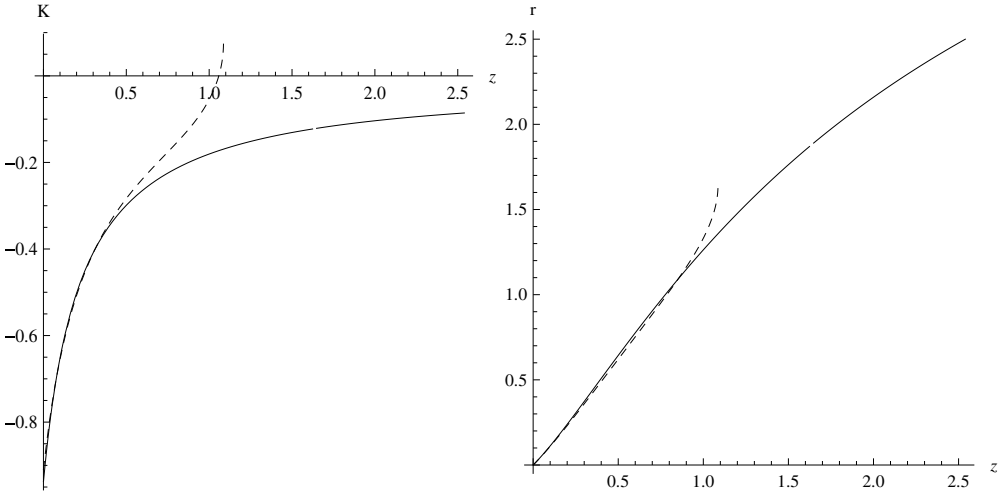

Figure 5. The curvature $K(z)$ and the comoving radial coordinate $r(z)$ are plotted as a function of the red-shift. The black dashed line corresponds to $K_0 = -0.91$ and the black line corresponds to $K_0 = -0.9376$. As it can be seen for $K_0 = -0.91$ there is critical red-shift after which r is decreasing, corresponding to a transition from red to blue-shift. This implies that this choice of the initial conditions is not compatible with the observed expansion of the Universe.

coordinates we have chosen a LTB solution is determined uniquely by the function $k(r)$, so we will have a total of three independent functions to solve for $\eta(z)$, $r(z)$, $k(z)$. Since we have already two differential equation for the geodesics, we need an extra differential equation.

This can be obtained by differentiating respect to the red-shift the luminosity distance $D_L(z)$

$$\frac{\mathrm{d}}{\mathrm{d}z}\left(\frac{D_L^{\mathrm{obs}}(z)}{(1+z)^2}\right) = \frac{\partial(ra(\eta,r))}{\partial\eta}\frac{\mathrm{d}\eta}{\mathrm{d}z} + \frac{\partial(ra(\eta,r))}{\partial r}\frac{\mathrm{d}r}{\mathrm{d}z} = s(z) \tag{36}$$

where $D_L^{\mathrm{obs}}(z)$ is the observed luminosity distance. In our case we will use the best fit ΛCDM function. Now we have the set of equations we were looking for

$$\frac{\mathrm{d}\eta}{\mathrm{d}z} = p(\eta(z), r(z)) = p(z), \tag{37}$$

$$\frac{\mathrm{d}r}{\mathrm{d}z} = q(\eta(z), r(z)) = q(z), \tag{38}$$

$$\frac{\mathrm{d}}{\mathrm{d}z}\left(\frac{D_L^{\mathrm{obs}}(z)}{(1+z)^2}\right) = s(z). \tag{39}$$

Since we will solve our differential equations respect to the variable z, we need to transform the partial derivatives respect to η and r in equations (15), (16) according to the chain rule:

$$\left.\frac{\partial h(\eta,r)}{\partial r}\right|_{(\eta=\eta(z),r=r(z))} = \frac{\partial h(\eta(z),r(z))}{\mathrm{d}z}\frac{\mathrm{d}z}{\mathrm{d}r}, \tag{40}$$

$$\left.\frac{\partial h(\eta,r)}{\partial \eta}\right|_{(\eta=\eta(z),r=r(z))} = \frac{\partial h(\eta(z),r(z))}{\mathrm{d}z}\frac{\mathrm{d}z}{\mathrm{d}\eta}, \tag{41}$$

where $h(\eta, r)$ is a generic function in the coordinates (η, r). After this substitution the equations contain only functions of the red-shift z, and derivatives respect to z. The differential equations obtained in this form need to be further manipulated in order to re-write them in a canonical form in which the derivatives appear all on one side, since after the application of the chain rule to equations (15), (16) derivative terms like $\frac{\mathrm{d}r(z)}{\mathrm{d}z}$, $\frac{\mathrm{d}\eta(z)}{\mathrm{d}z}$, $\frac{\mathrm{d}k(z)}{\mathrm{d}z}$ are also on the right-hand side. We can now use equations (40) and (41) in equations (37)–(39) and after a rather complicated algebraic manipulation we get:

$$\begin{aligned}
&2t^2\sqrt{K(z)}((6+4t^2)r(z) + (3+t^2)\sqrt{1-K(z)r(z)^2}T(z))K'(Z)\\
&\quad -12t^3\sqrt{1-K(z)r(z)^2}K'(Z) +\\
&\quad -8t^3(1+z)K(z)^2r'(z)T'[z] - 2tK(z)r(z)K'(z)(3(1+t^2)T(z)\\
&\quad +(3+5t^2)(1+z)T'(z))\\
&\quad +K(z)^{3/2}(-8t^4r'(z) + 3(1+t^2)^2(1+z)r(z)T(z)K'(z)T'(z)) = 0
\end{aligned} \tag{42}$$

$$\begin{aligned}
&r'(z)(2t(3+5t^2)(1+z)r(z)K'(z) - \sqrt{K(z)}(8t^4\sqrt{1-K(z)r(z)^2}\\
&\quad +3(1+t^2)^2(1+z)r(z)T(z)K(z)) + 8t^3(1+z)K(z)r'(z)) = 0
\end{aligned} \tag{43}$$

$$\begin{aligned}
&2K(z)((1+K_0)t^2r'(z) - (1+t^2)K(z)H_0\frac{\mathrm{d}}{\mathrm{d}z}\left(\frac{D_L^{\mathrm{obs}}(z)}{(1+z)^2}\right)) +\\
&\quad -(1+K_0)tr(z)((2t - \sqrt{K(z)}T(z))K(z) - 2K(z)^{3/2}T'(z)) = 0.
\end{aligned} \tag{44}$$

In the above expressions we have expressed all the trigonometric functions in terms of the equivalent expressions in terms of $\tan(X)$ according to

$$t = \tan(X), \tag{45}$$

$$X = \tfrac{1}{2}\sqrt{K(z)}T(z). \tag{46}$$

This is achieved by using a series of Mathetica simplifying routines developed for this purpose. We have also used the dimensionless version of the solution in terms of $K(z)$, $T(z)$ derived in the previous section.

As it can be seen the above three equations are not linear in the derivative terms, but the second one only involves $\{r'(z), K'(z)\}$, while the other two involve all the three functions $\{r'(z), K'(z), T'(z)\}$. This suggests that we can first solve for $r'(z)$ in terms of only $K'(z)$ from the equation (43):

$$\begin{aligned} r'(z) = \frac{1}{8t^3(1+z)K(z)}[&8t^4\sqrt{K(z)}\sqrt{1-K(z)r(z)^2} - 6tr(z)K'(z) - 10t^3r(z)K'(z) \\ &-6tzr(z)K'(z) - 10t^3zr(z)K'(z) + 3\sqrt{K(z)}r(z)T(z)K'(z) \\ &+6t^2\sqrt{K(z)}r(z)T(z)K'(z) + 3t^4\sqrt{K(z)}r(z)T(z)K'(z) \\ &+3z\sqrt{K(z)}r(z)T(z)K'(z) \\ &+6t^2z\sqrt{K(z)}r(z)T(z)K'(z) + 3t^4z\sqrt{K(z)}r(z)T(z)K'(z)] \end{aligned} \tag{47}$$

and then substitute in equations (42), (44) to get:

$$\begin{aligned} K'(z) = -\frac{1}{1+z}&t(12t^2(1+z)\sqrt{1-K(z)r(z)^2}K(z) - 2t(1+z)\sqrt{K(z)}(9(1+t^2)r(z) \\ &+(3+t^2)\sqrt{1-K(z)r(z)^2}T(z))K(z) + K(z)(8t^4\sqrt{1-K(z)r(z)^2} \\ &+3(3+4t^2+t^4)(1+z)r(z)T(z)K(z)) \\ &+8t^3(1+z)K(z)^{3/2}\sqrt{1-K(z)r(z)^2}T'(z)) \end{aligned} \tag{48}$$

$$\begin{aligned} T'(z) = \frac{1}{4t(1+z)}&(-6(1+K_0)t(1+3t^2)(1+z)r(z)K(z) \\ &+(1+K_0)\sqrt{K(z)}(8t^4\sqrt{1-K(z)r(z)^2} \\ &+(3+10t^2+3t^4)(1+z)r(z)T(z)K(z)) \\ &-8t(1+t^2)(1+z)K(z)^2H_0\frac{\mathrm{d}}{\mathrm{d}z}\left(\frac{D_L^{\mathrm{obs}}(z)}{(1+z)^2}\right) \\ &+8(1+K_0)t^2(1+z)K(z)^{3/2}r(z)T'(z)). \end{aligned} \tag{49}$$

These two equations now only involve $K'(z)$, $T'(z)$ in a linear form, so they can be solved directly, and then the result for $K'(z)$ can be substituted in the equation for $r'(z)$. After some rather cumbersome algebraic manipulations we finally get:

$$\begin{aligned} \frac{\mathrm{d}T(z)}{\mathrm{d}z} = \frac{2\sqrt{K(z)}}{3t(1+K_0)r(z)} \times \Bigg[&H_0\frac{\mathrm{d}}{\mathrm{d}z}\left(\frac{D_L^{\mathrm{obs}}(z)}{(1+z)^2}\right) \\ &+\frac{H_0\frac{\mathrm{d}}{\mathrm{d}z}\left(\frac{D_L^{\mathrm{obs}}(z)}{(1+z)^2}\right)(1+3t^2)\sqrt{K(z)}r(z)}{2(\sqrt{K(z)}r(z) - t\sqrt{1-K(z)r(z)^2})} - \frac{(1+K_0)t^3\sqrt{1-K(z)r(z)^2}}{(1+t^2)(1+z)K(z)^{3/2}}\Bigg], \end{aligned} \tag{50}$$

$$\frac{\mathrm{d}r(z)}{\mathrm{d}z} = -\frac{\sqrt{1-K(z)r(z)^2}}{3\mathrm{t}(\mathrm{t}^2\mathrm{X}-3\mathrm{t}+3\mathrm{X})} \times \left[\frac{H_0 \frac{\mathrm{d}}{\mathrm{d}z}\left(\frac{D_L^{\mathrm{obs}}(z)}{(1+z)^2}\right)K(z)(t(3+5t^2)-3(1+t^2)^2X)}{(1+K_0)(-\sqrt{K(z)}r(z)+t\sqrt{1-K(z)r(z)^2})}\right.$$
$$\left. + \frac{2\mathrm{t}^2(2\mathrm{t}^3-3\mathrm{t}^2\mathrm{X}+3\mathrm{t}-3\mathrm{X})}{(1+t^2)(1+z)\sqrt{K(z)}}\right], \tag{51}$$

$$\frac{\mathrm{d}K(z)}{\mathrm{d}z} = \frac{4t^2\sqrt{K(z)}\sqrt{1-K(z)r(z)^2}}{3(1+K_0)(1+t^2)(1+z)r(z)(t^2X-3t+3X)}$$
$$\times\left[\frac{H_0 \frac{\mathrm{d}}{\mathrm{d}z}\left(\frac{D_L^{\mathrm{obs}}(z)}{(1+z)^2}\right)(1+t^2)(1+z)K(z)^{3/2}}{-\sqrt{K(z)}r(z)+t\sqrt{1-K(z)r(z)^2}} - (1+K_0)t^2\right] \tag{52}$$

where

$$t = \tan(X), \tag{53}$$

$$X = \tfrac{1}{2}\sqrt{K(z)}T(z), \tag{54}$$

and we have used the dimensionless version of the solution in terms of $K(z)$, $T(z)$ derived in the previous section. The main advantage of these equations is that they are fully analytical, while other versions require a numerical integration of the Einstein's equations. In this form the central value both H_0 and K_0 can fixed arbitrarily, and the remaining initial condition for $T(z)$ are fixed according to equation (33). This makes them suitable both for numerical and analytical applications. In particular they can be used to expand locally the solutions around the apparent horizon corresponding to the maximum of $D_A(z) = \frac{D_L(z)}{(1+z)^2}$. We will report in the appendix the relations which can be used to obtain such an expansion.

6. Apparent horizon, $H(z)$ and CMB

As it can be easily seen the differential equations we need to solve become unstable around a critical vale of the red-shift z_c, where the angular diameter distance

$$D_A^{\Lambda CDM}(z) = \frac{1}{(1+z)^2} D_L^{\Lambda CDM}(z) \tag{55}$$

which we use as input for our differential equations reaches its maximum. This is only an apparent horizon, due to the fact that we are the using red-shift as the variable of the differential equations, not to a real singularity of the space-time. In order to overcame this critical point we follow these steps.

- Choose a point $z_c - \epsilon_1$ before the apparent horizon where the numerical inversion method is still sufficiently accurate and stable, and taking advantage of the fully analytical system of differential equations, Taylor expand $T(z)$, $r(z)$, $K(z)$.
- Extrapolate the obtained Taylor expansions to a point after $z_c + \epsilon_2$ after the apparent horizon, sufficiently far to avoid the numerical instability and minimize the relative error between the extrapolated $D^{\mathrm{LTB}}_{\mathrm{Taylor}}(z)$ and $D_L^{\mathrm{Obs}}(z)$.
- Use the extrapolated values at $z_c + \epsilon_2$ as the initial conditions for the numerical solution of the system of differential equations after the apparent horizon.

This method is quite effective, as it can be seen in the plot of the relative error in figure 2, and allows to obtain a very accurate solution up to very high red-shift. We can get significantly more accurate results than previous ones [10], even after the critical point, since the fully analytical expression of the equations we use allows to obtain a very accurate Taylor expansion near the critical point.

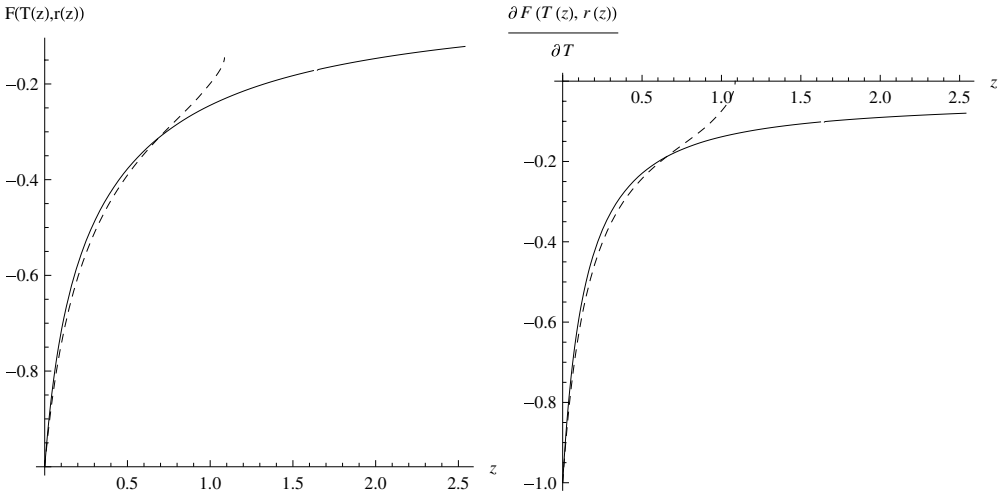

Figure 6. $F(T(z), r(z))$ and $\frac{\partial F(T(z),r(z))}{\partial T}$ are plotted as functions of the red-shift. Since $F(\eta, r) \propto \partial_r R(t(z), r(z))$ never crosses zero, no shell-crossing singularity appears along the past light cone. The point where $\frac{\partial F(T(z),r(z))}{\partial T}$ crosses zero corresponds to the transition from local expansion to local contraction, i.e from red to blue-shift. The dashed line corresponds to $K_0 = -0.91$ and the solid line corresponds to $K_0 = -0.9376$.

7. Application: blue to red-shift transition and $H_0(z_{LSS})$

As it can be seen in the figures the inversion procedure is quite accurate, since we can keep the relative error between the solution of the IP and $D_L^{\rm obs}(z)$ quite low, much better than in [10]. This is due to fact that the initial conditions we are setting are exact while in previous studies they were only approximate. Compared to [31] this method is more accurate because we expand in red-shift space the actual geodesics equation around the critical point.

We can now apply the inversion method we have derived. We find that only certain values of K_0 allow to solve the differential equations up to high red-shift. For sufficiently large K_0 we find in fact that the geodesics equations became unstable because we approach a point along the light cone where

$$\frac{\mathrm{d}z}{\mathrm{d}r} = 0 \tag{56}$$

i.e. there is a turning point from red-shift to blue-shift. This implies that these models are inconsistent with observations. As it can be seen from the geodesics equations this can happen when:

$$\partial_\eta F(\eta, r) = 0, \tag{57}$$

which in the (t, r) coordinates is equivalent to

$$\dot{R}'(t, r) = 0. \tag{58}$$

As shown in figure 6 this is exactly what occurs for certain values of K_0, where we can also see that this is not a shell-crossing singularity, since $F(\eta, r)$ never crosses zero before that point. We can easily interpret this result using our intuition about the Friedman like equation in which the Einstein's equations can be written for the LTB solution. The curvature term has to be negative in order to mimic the effects of a cosmological constant, and if the central value is not sufficiently large than there can be some critical point where the matter gravitational attraction will dominate and cause a contraction.

Another important observable to fit is the CMB spectrum. Since the CMB physics is determined by $H^{\rm LTB}(z_{LSS})$ it would be interesting to explore the possibility that an appropriate choice of K_0 could also give a good agreement between $H^{\rm LTB}(z_{LSS})$ and $H^{\Lambda CDM}(z_{LSS})$. The numerical solution of the IP shows that $H^{\rm LTB}(z_{LSS})$ is not affected significantly by K_0 and that a mismatch of the order of the 20% cannot be avoided, independently of the value of K_0. This implies than even taking into account the freedom on the choice of K_0 we cannot find any model such that

$$D_L^{\rm LTB}(z) = D_L^{\Lambda CDM}, \tag{59}$$

$$H^{\rm LTB}(z_{LSS}) = H^{\Lambda CDM}(z_{LSS}). \tag{60}$$

We deduce that none of these models should be able fit both $D_L(z)$ and the CMB spectrum, and it would be necessary the introduction of an extra functional degree of freedom, the bang function $t_b(r)$, to achieve that goal. Since we have explored all the possible set of initial conditions for $K(z)$, it should be noted that our conclusion is more general than previous ones based on particular choice of K_0.

The reason is that the $K(z)$ solution is asymptotically constant (zero in our case since we mimic a flat FLRW model) because at sufficiently high red-shift, where the cosmological constant is subdominant, the homogenous FLRW Universe has to be recovered. This implies that the low red-shift disagreement between $H^{\rm LTB}$ and $H^{\rm FLRW}$ remain the same at high red-shift, and in general they don't intersect, as long as we keep solving the IP for $D_L(z)$ at any red-shift.

8. Conclusions

We have developed a new fully analytical inversion method to map the observed luminosity distance to a LTB model. This method has the advantage of not requiring any numerical integration of the Einstein's equations, and is particularly suitable to obtain a Taylor expansion of the solution around the numerical instability point corresponding to the apparent horizon. The accuracy of the solution we obtain significantly improves previous methods, because we are able to fix exactly initial conditions and the Taylor expansion in red-shift is very precise, allowing to overcame the apparent horizon keeping the relative error low.

We have tested this inversion method to investigate the importance of the choice of the initial central value K_0 for the curvature function defining the LTB model. We found that only a certain range of values is consistent with the observed cosmic red-shift, since higher values of K_0 lead to a transition from red to blue-shift. We have also checked that the high red-shift value of $H^{\rm LTB}$ is not affected significantly by K_0, and that all the acceptable models, i.e. the ones without blue to red-shift transition, have a disagreement of the order of 20% respect to $H^{\Lambda CDM}(z_{LSS})$. Since we have explored all the possible set of initial conditions for $K(z)$, it should be noted that our conclusion is more general than previous ones based on a particular choice of K_0 or ansatz for some of the functions defining the LTB model. In the future it will be interesting to extend this method to the case of a not vanishing bang function $t_b(r)$ in order to solve the inversion problem also for the Hubble parameter as a function for the red-shift.

The method we developed does not need to be applied to LTB metrics as cosmological models describing the local universe around us, but could be applied to study the effects of large scale inhomogeneities for a generic observer located inside some region of the Universe corresponding to a local overdensity or underdensity which cannot be modeled simply perturbation of a FLRW metric.

Acknowledgments

Chen and Romano are supported by the Taiwan NSC under Project no. NSC97-2112-M-002-026-MY3, by Taiwan's National Center for Theoretical Sciences (NCTS). Chen is also supported by the US Department of Energy under Contract no. DE-AC03-76SF00515. AER is also supported by UDEA under the programs GFIF Sostenibilidad, dedicacion exclusica and the CODI project IN10219CE.

Appendix. Expansion around the apparent horizon

In this appendix we give an explicit form of the coefficients of the expansion of the geodesics equation around the apparent horizon z_c. The linear coefficients are simply given by evaluating the right-hand side of the geodesics equations at z_c. Since the right-hand side of the geodesics equations is fully analytical, we can take its first derivative, and then solve for the second derivative terms to obtain:

$$\frac{\mathrm{d}^2K(z)}{\mathrm{d}z^2}\frac{\mathrm{d}\ln K(z)}{\mathrm{d}z}\left[\frac{\mathrm{d}\ln(1-K(z)r(z)^2)}{2K(z)r(z)^2\mathrm{d}z}+\frac{\mathrm{d}\ln K(z)}{\mathrm{d}z}-\frac{1}{1+z}+\frac{\mathrm{d}\ln(K(z)r(z)^2)}{\mathrm{d}z}\right.$$
$$\left.\times\left(\frac{2X}{t}+\frac{2t(t-X)X}{3t-(3+t^2)X}\right)+\frac{H_0\frac{\mathrm{d}^2}{\mathrm{d}z^2}\left(\frac{D_L^{\mathrm{obs}}(z)}{(1+z)^2}\right)(1+t^2)(1+z)K(z)}{(1+K_0)t^2(1-t\sqrt{K(z)^{-1}r(z)^{-2}-1})r(z)}\right], \tag{A.1}$$

$$\frac{\mathrm{d}^2r(z)}{\mathrm{d}z^2}=\frac{\mathrm{d}\ln r(z)}{\mathrm{d}z}\left[\frac{\mathrm{d}\ln(1-K(z)r(z)^2)}{2K(z)r(z)^2\mathrm{d}z}+\frac{\mathrm{d}\ln r(z)}{\mathrm{d}z}-\frac{1}{1+z}+\frac{X\mathrm{d}\ln(K(z)r(z)^2)}{3\mathrm{d}z}\right.$$
$$\times\left(\frac{3+t^2}{2t}+\frac{2t^3X}{3t-(3+t^2)X}+\frac{3t^4}{t(3+2t^2)-3(1+t^2)X}\right)-\frac{H_0(1+z)}{1+K_0}$$
$$\left.\times\frac{\frac{\mathrm{d}^2}{\mathrm{d}z^2}\left(\frac{D_L^{\mathrm{obs}}(z)}{(1+z)^2}\right)(1+t^2)K(z)}{t^2(1-t\sqrt{K(z)^{-1}r(z)^{-2}-1})r(z)}\left(1+\frac{3t^3-3(1+t^2)t^2X}{t(3+2t^2)-3(1+t^2)X}\right)\right], \tag{A.2}$$

$$\frac{\mathrm{d}^2T(z)}{\mathrm{d}z^2}=\frac{\mathrm{d}\ln T(z)}{\mathrm{d}z}\left[\frac{\mathrm{d}\ln(1-K(z)r(z)^2)}{2K(z)r(z)^2\mathrm{d}z}-\frac{\mathrm{d}\ln K(z)}{2\mathrm{d}z}-\frac{1}{1+z}+\frac{X\mathrm{d}\ln(K(z)r(z)^2)}{t\mathrm{d}z}\right.$$
$$\left.-\frac{H_0\frac{\mathrm{d}^2}{\mathrm{d}z^2}\left(\frac{D_L^{\mathrm{obs}}(z)}{(1+z)^2}\right)(1+t^2)(1+z)K(z)^{3/2}}{2(1+K_0)t^3\sqrt{1-K(z)r(z)^2}}\left(2+\frac{1+3t^2}{1-t\sqrt{K(z)^{-1}r(z)^{-2}-1}}\right)\right]. \tag{A.3}$$

The derivation of the these coefficients is taking into account that $D_A'(z_c)=0$ and involves a series of cumbersome algebraic and trigonometric manipulations of the type used in the derivation of the inversion equations, which have been carried out using a set of routines written in MATHEMATICA for this specific purpose.

References

[1] Riess A G *et al* 1998 *Astron. J.* **116** 1009 (arXiv:astro-ph/9805201)
[2] Perlmutter S *et al* 1999 *Astrophys. J.* **517** 565 (arXiv:astro-ph/9812133)

[3] Tonry J L *et al* 2003 *Astrophys. J.* **594** 1 (arXiv:astro-ph/0305008)
[4] Knop R A *et al* 2003 *Astrophys. J.* **598** 102 (arXiv:astro-ph/0309368)
[5] Barris B J *et al* 2004 *Astrophys. J.* **602** 571 (arXiv:astro-ph/0310843)
[6] Riess A G *et al* 2004 *Astrophys. J.* **607** 665 (arXiv:astro-ph/0402512)
[7] Bennett C *et al* (WMAP Collaboration) 2003 *Astrophys. J. Suppl.* **148** 1 (arXiv:astro-ph/0302207)
[8] Spergel D *et al* (WMAP Collaboration) 2007 *Astrophys. J. Suppl.* **170** 377 (arXiv:astro-ph/0603449)
[9] Romano A E 2007 *Phys. Rev.* D **75** 043509 (arXiv:astro-ph/0612002)
[10] Chung D J and Romano A E 2006 *Phys. Rev.* D **74** 103507 (arXiv:astro-ph/0608403)
[11] Yoo C-M, Kai T and Nakao K-i 2008 *Prog. Theor. Phys.* **120** 937 (arXiv:0807.0932)
[12] Romano A E 2010 *J. Cosmol. Astropart. Phys.* JCAP05(2010)020 (arXiv:0912.2866)
[13] Alexander S, Biswas T, Notari A and Vaid D 2009 *J. Cosmol. Astropart. Phys.* JCAP09(2009)025 (arXiv:0712.0370)
[14] Alnes H, Amarzguioui M and Gron O 2006 *Phys. Rev.* D **73** 083519 (arXiv:astro-ph/0512006)
[15] Garcia-Bellido J and Haugboelle T 2008 *J. Cosmol. Astropart. Phys.* JCAP04(2008)003 (arXiv:0802.1523)
[16] Garcia-Bellido J and Haugboelle T 2008 *J. Cosmol. Astropart. Phys.* JCAP09(2008)016 (arXiv:0807.1326)
[17] Garcia-Bellido J and Haugboelle T 2009 *J. Cosmol. Astropart. Phys.* JCAP09(2009)028 (arXiv:0810.4939)
[18] Romano A E 2012 *Int. J. Mod. Phys.* D **21** 1250085 (arXiv:1112.1777)
[19] February S, Larena J, Smith M and Clarkson C 2010 *Mon. Not. R. Astron. Soc.* **405** 2231 (arXiv:0909.1479)
[20] Romano A E 2010 *J. Cosmol. Astropart. Phys.* JCAP01(2010)004 (arXiv:0911.2927)
[21] Clarkson C, Cortes M and Bassett B A 2007 *J. Cosmol. Astropart. Phys.* JCAP08(2007)01 (arXiv:astro-ph/0702670)
[22] Ishibashi A and Wald R M 2006 *Class. Quantum Grav.* **23** 235 (arXiv:gr-qc/0509108)
[23] Bolejko K, Hellaby C and Alfedeel A H 2011 *J. Cosmol. Astropart. Phys.* JCAP09(2011)011 (arXiv:1102.3370)
[24] Romano A E 2013 *Gen. Rel. Grav.* **45** 1515 (arXiv:1206.6164)
[25] Clifton T, Ferreira P G and Zuntz J 2009 *J. Cosmol. Astropart. Phys.* JCAP07(2009)029 (arXiv:0902.1313)
[26] Romano A E 2007 *Phys. Rev.* D **76** 103525 (arXiv:astro-ph/0702229)
[27] Balcerzak A and Dabrowski M P 2013 arXiv:1310.7231
[28] Zibin J P 2011 *Phys. Rev.* D **84** 123508 (arXiv:1108.3068)
[29] Bull P, Clifton T and Ferreira P G 2012 *Phys. Rev.* D **85** 024002 (arXiv:1108.2222)
[30] Romano A E 2010 *Phys. Rev.* D **82** 123528 (arXiv:0912.4108)
[31] Celerier M-N, Bolejko K and Krasinski A 2010 *Astron. Astrophys.* **518** A21 (arXiv:0906.0905)
[32] Iguchi H, Nakamura T and Nakao K-i 2002 *Prog. Theor. Phys.* **108** 809 (arXiv:astro-ph/0112419)
[33] Yoo C-M 2010 *Prog. Theor. Phys.* **124** 645 (arXiv:1010.0530)
[34] Clarkson C and Regis M 2011 *J. Cosmol. Astropart. Phys.* JCAP02(2011)013 (arXiv:1007.3443)
[35] Lim W C, Regis M and Clarkson C 2013 *J. Cosmol. Astropart. Phys.* JCAP10(2013)010 (arXiv:1308.0902)
[36] Romano A E, Sasaki M and Starobinsky A A 2012 *Eur. Phys. J.* C **72** 2242 (arXiv:1006.4735)
[37] Romano A E and Chen P 2012 arXiv:1207.5572
[38] Romano A E and Chen P 2011 *Int. J. Mod. Phys.* D **20** 2823 (arXiv:1208.3911)
[39] Romano A E, Sanes S and Sasaki M 2013 arXiv:1311.1476
[40] Romano A E 2012 arXiv:1204.0866
[41] Romano A E and Vallejo S A 2014 arXiv:1403.2034
[42] Zibin J P and Moss A 2011 *Class. Quantum Grav.* **28** 164005 (arXiv:1105.0909)
[43] Zhang P and Stebbins A 2011 *Phys. Rev. Lett.* **107** 041301 (arXiv:1009.3967)
[44] Bester H L, Larena J, van der Walt P J and Bishop N T 2014 *J. Cosmol. Astropart. Phys.* JCAP02(2014)009 (arXiv:1312.1081)
[45] Lemaitre G 1997 *Gen. Rel. Grav.* **29** 641
[46] Tolman R C 1934 *Proc. Natl Acad. Sci. USA* **20** 169
[47] Bondi H 1947 *Mon. Not. R. Astron. Soc.* **107** 410
[48] Romano A E and Sasaki M 2012 *Gen. Rel. Grav.* **44** 353 (arXiv:0905.3342)